Accepted Manuscript

Hypoxia augments LPS-induced inflammation and triggers high altitude cerebral edema in mice

Yanzhao Zhou, Xin Huang, Tong Zhao, Meng Qiao, Xingnan Zhao, Ming Zhao, Lun Xu, Yongqi Zhao, Liying Wu, Kuiwu Wu, Ruoli Chen, Ming Fan, Lingling Zhu

PII: S0889-1591(17)30115-0
DOI: http://dx.doi.org/10.1016/j.bbi.2017.04.013
Reference: YBRBI 3126

To appear in: *Brain, Behavior, and Immunity*

Received Date: 29 December 2016
Revised Date: 6 March 2017
Accepted Date: 17 April 2017

Please cite this article as: Zhou, Y., Huang, X., Zhao, T., Qiao, M., Zhao, X., Zhao, M., Xu, L., Zhao, Y., Wu, L., Wu, K., Chen, R., Fan, M., Zhu, L., Hypoxia augments LPS-induced inflammation and triggers high altitude cerebral edema in mice, *Brain, Behavior, and Immunity* (2017), doi: http://dx.doi.org/10.1016/j.bbi.2017.04.013

Hypoxia augments LPS-induced inflammation and triggers high altitude cerebral edema in mice

Yanzhao Zhou[1#], Xin Huang[1#], Tong Zhao[1], Meng Qiao[1], Xingnan Zhao[1], Ming Zhao[1], Lun Xu[1], Yongqi Zhao[1], Liying Wu[1], Kuiwu Wu[1], Ruoli Chen[4], Ming Fan[1,2,3*], Lingling Zhu[1,2*]

1. Department of Cognitive Sciences, Institute of Basic Medical Sciences, Beijing, China
2. Co-Innovation Center of Neuroregeneration, Nantong University, Nantong, China
3. Beijing Institute for Brain Disorder, Beijing, China
4. School of Pharmacy, Keele University, Staffordshire ST5 5BG, UK

[#] Co-first authors

* Corresponding authors

Correspondence information for corresponding authors:

Lingling Zhu, MD, Ph.D.

Department of Cognitive Sciences,

Beijing Institute of Basic Medical Sciences, Beijing, China;

No. 27 Taiping Rd, Beijing 100850, P.R. China

Phone: 86-10-68210077 ext. 931315

Fax: 86-10-68213039

Email: linglingzhu@hotmail.com

or

Professor Ming Fan

Department of Cognitive Sciences,

Beijing Institute of Basic Medical Sciences, Beijing, China;

No. 27 Taiping Rd, Beijing 100850, P.R. China

Phone: 86-10-68210077 ext. 932333

Fax: 86-10-68213039

Email: fanming@nic.bmi.ac.cn

Co-authors' email addresses:

Yanzhao Zhou: whuzhouyanzhao@163.com; Xin Huang: huangxin1010@163.com; Tong Zhao: zhaotongj@sohu.com; Meng Qiao: qiaomeng0730@163.com; Xingnan Zhao: 1360824558@qq.com; Ming Zhao: zhaoming1981@163.com; Lun Xu: lunlunxu@163.com; Yongqi Zhao: zhaoyq777@163.com; Liying Wu: wuliying985@hotmail.com; Kuiwu Wu: ammswu@sina.com;

Ruoli Chen: r.chen@keele.ac.uk; Ming Fan: fanmingchina@126.com; Lingling Zhu: linglingzhu@hotmail.com

Abstract

High altitude cerebral edema (HACE) is a life-threatening illness that develops during the rapid ascent to high altitudes, but its underlying mechanisms remain unclear. Growing evidence has implicated inflammation in the susceptibility to and development of brain edema. In the present study, we investigated the inflammatory response and its roles in HACE in mice following high altitude hypoxic injury. We report that acute hypobaric hypoxia induced a slight inflammatory response or brain edema within 24 h in mice. However, the lipopolysaccharide (LPS)-induced systemic inflammatory response rapidly aggravated brain edema upon acute hypobaric hypoxia exposure by disrupting blood-brain barrier integrity and activating microglia, increasing water permeability via the accumulation of aquaporin-4 (AQP4), and eventually leading to impaired cognitive and motor function. These findings demonstrate that hypoxia augments LPS-induced inflammation and induces the occurrence and development of cerebral edema in mice at high altitude. Here, we provide new information on the impact of systemic inflammation on the susceptibility to and outcomes of HACE.

Key words: lipopolysaccharide (LPS), blood-brain barrier (BBB), high altitude cerebral edema (HACE), inflammation

1. Introduction

High altitudes and mountains cover one-fifth of the earth's surface. With advances in technology, millions of people travel to high altitude areas for recreational, religious, economic and military purposes (Gallagher and Hackett, 2004). High altitude is characterized by hypobaric hypoxia, decreased temperatures, lower humidity and increased ultraviolet radiation (Gallagher and Hackett, 2004; Netzer et al., 2013). Among these factors, hypobaric hypoxia is regarded as the main factor contributing to altitude-related illness, which is quite common in those who are not adequately acclimated (MacInnis et al., 2010; Rodway et al., 2003; Bailey et al., 2009). Altitude-related illnesses include acute mountain sickness (AMS), high altitude pulmonary edema (HAPE) and high altitude cerebral edema (HACE). Among these, HACE is the most serious and can be lethal (Gallagher and Hackett, 2004; Eide and Asplund, 2009). HACE often occurs in those who abruptly ascend to over

3,000 m, but the lowest reported altitude known to induce HACE was 2,100 m (Dickinson, 1979). The prevalence of HACE is estimated to be 0.5 to 1% among persons at altitudes of 4,000-5,000 m (Bärtsch and Swens. 2013). HACE is regarded as the end-stage of AMS and is characterized by truncal ataxia and decreased consciousness. If the appropriate treatment is not received within a certain period of time, coma may evolve, followed by death within 24 h due to brain herniation (Hackett and Roach. 2001). However, the mechanisms that cause HACE symptoms remain elusive, and methods for the prevention and treatment of HACE are limited (Guo et al., 2014).

Inflammation plays important roles in many diseases. High altitude exposure is often associated with gastrointestinal disorders, inflammation and increased risk of infection (Kleessen et al., 2005). It was reported that the incidence of digestive system disease is quite high among high altitude residents and immigrants (Recavarren et al., 2005). A markedly higher incidence of AMS in mountaineers with respiratory or gastrointestinal infections has also been reported (Murdoch, 1995). Murdoch also identified that the frequency of infectious symptoms was positively related to Lake Louise scores. A retrospective study in Colorado reported that 79% of HAPE patients had preexisting inflammation-inducing illness (Durmowicz, 1997). In viral infections, pulmonary edema is induced by hypoxia (Carpenter et al., 1998). It was recently reported that plasma TNF-α, IL-1β and IL-6 levels significantly increased when volunteers ascended to an altitude of 3860 m. A growing number of reports have also shown that inflammation plays a vital role in altitude-related illness (Song et al., 2016). However, the relationship between inflammation and HACE has been rarely investigated.

In the present study, we first investigated the potential role of systemic inflammation in the development of HACE. We found that acute hypobaric hypoxia (AHH) exposure significantly augmented lipopolysaccharide (LPS)-induced systemic inflammation. Cerebral edema, blood brain barrier (BBB) disruption, and neurological injury were induced after pretreatment with low doses of LPS followed by AHH exposure, whereas neither low-dose LPS injection nor AHH exposure alone induced marked effects. These results indicate that systemic inflammation induced by LPS aggravates brain edema under AHH exposure by disrupting BBB integrity and activating microglia, thus causing an accumulation of aquaporin-4 (AQP4) that increases water permeability and leads to impaired cognitive and motor function in mice. These findings demonstrate that the inflammatory response plays vital roles in the occurrence and development of HACE and provide a novel and efficient HACE mouse model for further studies.

2. Materials and methods

2.1 Animals

Male adult 8-week-old C57BL/6 mice were supplied by the Vital River Experimental Animal Company, Beijing. Animals were maintained in the animal house of the Beijing Institute of Basic Medical Sciences and were housed at a constant temperature under a 12-h light-dark cycle with unlimited access to standard diet and water. The animal protocol was approved by the Institutional Animal Care and Use Committee of the Institute of Basic Medical Sciences.

2.2 LPS administration and AHH exposure

For LPS administration, the mice were subjected to an intraperitoneal injection of a certain concentration of LPS (*Escherichia coli* 055:B5; Sigma-Aldrich, USA) diluted in natural salt water. For AHH exposure, the mice were placed in a decompression chamber (model: DYC-DWI; Fenglei, China) and subjected to hypobaric hypoxia equal to a height of 6,000 m (369.4 mmHg, equal to 10.16% O_2) at the velocity of 50 m/s in 5 min) for various durations. Animals receiving both treatments were subjected to LPS administration first. Thirty min later, the animals showed inflammatory symptoms and were then subjected to hypobaric hypoxia exposure.

2.3 Serum ELISA

Blood samples were clotted for 2 h at room temperature before centrifuging for 20 min at 2,000 g. Serums were aliquoted and stored at -80°C. The concentrations of IL-1β, IL-6, and TNF-α were determined using a Quantikine ELISA kit (R&D systems, USA) according to the manufacturer's protocol. The results are shown as the concentration of cytokines per milliliter serum.

2.4 Real-time PCR

Total RNA was extracted from the hippocampus of the mouse brains using TRIzol reagent (Invitrogen, USA). First-stand cDNA of each sample was synthesized using an MLV reverse transcription kit (TAKARA, Japan) according to the manufacturer's instructions. The cDNA was used as a template for quantitative real-time PCR using the SYBR green master mix (Applied Biosystems, USA). Gene expression was calculated relative to β-actin. The primers used were as follows: IL-1β: forward: 5'-TGCAACTGTTCCTGAACTCAACT-3', reverse: 5'-ATCTTTTGGGGTCCGTCAACT-3'; IL-6: forward: 5'-TAGTCCTTCCTACCCCAATTTCC-3', reverse: 5'-TTGGTCCTTAGCCACTCCTTC-3'; TNF-α: forward: 5'-CCCTCACACTCAGATCATCTTCT-3', reverse:

5'-GCTACGACGTGGGCTACAG-3'; MCP-1: forward: 5'-TTAAAAACCTGGATCGGAACCAA-3', reverse: 5'-GCATTAGCTTCAGATTTACGGGT-3'; ICAM: forward: 5'-GTGATGCTCAGGTATCCATCCA-3', reverse: 5'-CACAGTTCTCAAAGCACAGCG-3'; VCAM: forward: 5'-AGTTGGGGATTCGGTTGTTCT-3', reverse: 5'-CCCCTCATTCCTTACCACCC-3'; β-actin: forward: 5'-GGCTGTATTCCCCTCCATCG-3', reverse: 5'-CCAGTTGGTAACAATGCCATGT-3'.

2.5 Determination of brain water content (BWC)

Mice were anesthetized with 1% sodium pentobarbital. For each mouse, the brain was removed and its wet weight was determined using a precision electronic balance (BSA124S-CW; Sartorius, Germany). The brains were then placed in an oven and baked at 100°C for 48 h until a constant weight was obtained. The percentage of BWC was calculated as follows: BWC (%) = (wet weight - dry weight)/wet weight × 100%.

2.6 Magnetic resonance imaging (MRI)

MRI was conducted using the laboratory animal imagine analysis platform, Institute of Laboratory Animal Sciences, China Academy of Medical Sciences. Each mouse was anesthetized with isoflurane, fixed in a body restrainer and placed in an MRI spectrometer (Varian, USA). T2-multiecho images were acquired using a spin-echo sequence with the following parameters: 5 contiguous coronal slices at 2-mm thickness, 40 × 40 mm field of view, 128 × 128 matrix, repetition time (TR) = 2,000 ms, echo time (TE) = 36.00 ms. To map the apparent diffusion coefficient (ADC) of water, diffusion-weighted images were acquired with a spin-echo sequence. Five contiguous coronal slices were acquired (2-mm thick, 40 ×40 mm field of view, 128 × 128 matrix, TR = 2,000 ms, TE = 36.00 ms). ADC maps were automatically calculated according to the following equation: ADC = ln(S0/S1)/(b1 − b0) (mm^2/s). After exposure to hypoxia, the mice were immediately placed in an MRI scanner (VARIAN) for ADC measurements and imaging.

2.7 Immunofluorescence staining

The mice were anesthetized and perfused with 4% paraformaldehyde. The brains were isolated, dehydrated and frozen sectioned. The sections were blocked with 5% donkey serum (0.3% PBST, containing 5% donkey serum and 5% BSA) and incubated with specific primary (GFAP 1:500, DAKO or Iba-1 1:200, WAKO) and secondary antibodies (Alexa Fluor 594 conjugated 1:200, Life). Images were captured using a scanning confocal microscope (Nikon, Japan) and analyzed with Image J

software.

2.8 Western blot

Total protein was extracted from the mouse hippocampus. Samples were denatured and loaded on sodium dodecyl sulfate-polyacrylamide gels. Then, the proteins were transferred to a nitrocellulose membrane and blocked in 5% non-fat milk. The specific primary antibody (zonulae occludentes (ZO)-1 1:1,000 Invitrogen, VE-cadherin 1:1,000 eBioscience, occludin 1:1,000 Invitrogen, claudin-5 1:1,000 Thermo, VEGF 1:1,000 Abcam, AQP-4 1:8,000 Proteintech, or β-actin 1:10,000 Sigma) was applied overnight at 4°C, followed by incubation with HRP-conjugated goat-anti-mouse or goat-anti-rabbit antibodies (Bio-Rad, USA). The specific bands were detected using an ECL detection system (Bio-Rad, USA).

2.9 Determination of BBB permeability

Each mouse was subjected to an intraperitoneal injection of Evans blue dissolved in natural salt water (4 mg/kg of body weight) 24 h before the experiment. After AHH exposure, each mouse was anaesthetized and perfused. The brain was removed and dissolved in formamide and water-bathed at 55°C overnight. The samples were centrifuged at 12,000 × g at room temperature for 30 min. The supernatants were transferred to a 96-well plate, and the absorbance at 620 nm was determined.

Auto-fluorescence of Evans blue was evaluated as previously reported (Zuo et al., 2016). After AHH exposure, each mouse was anaesthetized and sacrificed. The brain was removed and immersed in 4% paraformaldehyde. Then, the brain tissue was cut into 40-μm coronal floating sections. The red auto-fluorescence of Evans blue was observed under a fluorescence microscope (Olympus, Japan).

2.10 Transmission electron microscopy

The preparation of samples for transmission electron microscopy was performed as previously described. The mice were anesthetized and the hippocampus was removed and immersed in glutaraldehyde. Ultra-microstructures were visualized and captured using a transmission electronic microscope (Hitachi, Japan).

2.11 Hematoxylin-eosin (HE) and Nissl staining

The mice were anesthetized. The brains were isolated and sectioned. The sections were immersed in absolute ethyl alcohol, 95% ethyl alcohol, and 70% ethyl alcohol for 1 min at room temperature and then incubated in cresyl violet for 30 min at 37°C. Then, the sections were subjected to dehydration and visualized with a microscope (Olympus, Japan).

2.12 Analysis of neuron morphology

Thy1-YFP mice were anesthetized and perfused according to the protocol above. The brains were post-fixed, followed by dehydration and cut in the coronal plane in 40-μm-thick sections. The sections were visualized with a scanning confocal microscope (Nikon, Japan), and representative images were captured.

2.13 Morris water maze test

The water maze was constructed using a black circular pool of 122 cm in diameter that was divided into 4 equal quadrants. A transparent circular platform (10 cm^2) was submerged 1.5 cm beneath the water surface. The water temperature was kept at 19-22°C. The swimming path of each animal was recorded using a video camera and analyzed using a professional analysis system (ANY-maze system, UK). Training was performed for 5 successive days with a platform beneath the water. After 5 days of training, the mice were subjected to LPS injection, AHH exposure or both on the 6^{th} day. The platform was removed from the pool, and the trials were begun to determine spatial learning and memory differences.

2.14 Rota-rod test

A Rota-rod test was conducted as previously described (Morris et al., 2013). The mice were trained to walk to stay on the rod rotating from 4 to 40 rpm over 300 s 3 times a day for 2 consecutive days. The mice were tested on the 3^{rd} day immediately after LPS injection, AHH exposure, or both. The latency and rotating speed at which the mice fell off the rotating rod were recorded.

2.15 Statistical analysis of the data

All experiments were repeated at least 3 times. The data are presented as the group mean values with standard errors of the means (SEM). Asterisks indicate significant differences between groups according to the Student's t-test or one-way analysis of variance (ANOVA). For all analyses, $p < 0.05$ was considered significant.

3. Results

3.1 AHH alone induces a slight inflammatory response and brain edema in mice

To explore whether exposure to AHH induced inflammation at the early stage of the ascent to the plateau, adult mice were exposed to a decompression chamber mimicking an altitude of 6,000 m (equivalent to 10.16% O_2 at sea level) for 6 h, 12 h and 24 h to acutely induce hypoxic brain injury. We

then examined changes in the pro-inflammatory cytokines IL-1β, IL-6 and TNF-α after exposure to AHH. Real-time PCR and ELISA were used to measure the gene expression and concentrations of these cytokines. The results indicated that AHH exposure did not affect the levels of IL-1β and TNF-α in the serum at 6 h but slightly down-regulated the level of IL-6, whereas the expression levels of these cytokines were not changed in the brain tissue at 6 h compared to normoxic controls (Fig. 1A-F). After 12 h of exposure to AHH, in the serum, the level of IL-1β increased from undetectable to 2 pg/ml, and IL-6 increased 2-fold, but no change in TNF-α was observed (Fig. 1A-C). The gene expression of IL-1β and IL-6 remained stable, but that of TNF-α increased by 2.7-fold in the brain tissue in mice exposed to AHH compared to controls (Fig. 1D-F). Twenty-four hours after exposure to AHH, in the serum, the level of IL-1β increased from undetectable to 3.8 pg/ml, the level of IL-6 increased by 2.6-fold ($p < 0.05$), and the gene expression in the brain of IL-1β, IL-6 and TNF-α were also elevated by 2.1-fold, 1.7-fold and 4.1-fold, respectively ($p < 0.05$) compared with the controls (Fig. 1A-F). Then, we examined the changes in the BWC at 6 h, 12 h and 24 h after AHH exposure as a sign of brain swelling. BWC did not increase at 6 h or 12 h after AHH exposure (Fig. 1G). There was only a slight, non-significant, increase from 78.43 ± 0.07% to 78.47 ± 0.13% at 24 h after AHH exposure. These data indicate that hypobaric hypoxia exposure alone induces a slight inflammatory response and brain edema in mice, which is consistent with our previous report (Huang et al., 2015).

3.2 LPS-induced systemic inflammation is amplified and rapidly induces the onset of brain edema in mice after AHH exposure

To further investigate the potential role of inflammation in the development of brain edema after AHH exposure, mice were intraperitoneally injected with LPS to promote systemic inflammation, and the possible mechanisms of LPS-induced inflammation under hypoxia were then investigated. We first compared the changes in BWC of mice injected with different concentrations of LPS (0, 0.1, 0.5, 1, 2.5, 5 and 10 mg/kg body weight) with or without AHH exposure for 6 h. As shown in Fig. 2A, a single injection of LPS from 0.1 to 5 mg/kg for 6 h did not increase BWC in mice. However, BWC was significantly increased in LPS-treated mice exposed to hypobaric hypoxia for 6 h compared with controls. This suggests that AHH exposure combined with LPS administration markedly induced cytotoxic or vasogenic edema compared with hypoxic exposure alone in mice. To reduce or prevent acute brain injury damage due to LPS administration, mice were injected with a lower dose of LPS (0.5

mg/kg, BW) for 6 h to induce the formation of HACE in the subsequent experiment. To confirm brain edema in this model, the ADC in the brain was detected by MRI. There was a significant increase in the cortical ADC value between the control group and the group treated with LPS injection combined with AHH exposure for 6 h (Fig. 2B-C). We further investigated the inflammatory response in LPS-induced inflammation after AHH exposure. First, compared to the normoxia control condition, AHH exposure alone for 6 h did not increase the levels of IL-1β, IL-6 and TNF-α in the serum (Fig. 2D-F) or the gene expression levels of IL-1β, IL-6 and TNF-α in the cortex (Fig. 2J-L). A single injection of LPS (0.5 mg/kg, BW) induced a systemic pro-inflammatory response for 6 h in mice. The level of IL-1β increased from undetectable to 16 pg/ml, and 88.7-fold and 3.9-fold increases in the levels of IL-6 and TNF-α, respectively, were also observed in the serum. Combined with AHH exposure, IL-1β levels increased from undetectable to 40 pg/ml, and the levels of IL-6 and TNF-α increased by 687.5-fold and 12-fold, respectively, in the serum (Fig. 2D-F). Pro-inflammatory cytokines stimulate endothelial cells to produce chemokines such as MCP-1 and cell adhesion molecules such as ICAM and VCAM, thus promoting leukocyte infiltration and neuroinflammation induction. LPS injection induced the up-regulation of MCP-1, ICAM and VCAM by 7.9-fold, 3.3-fold and 1.4-fold, respectively. When LPS injection was combined with AHH exposure, MCP-1, ICAM and VCAM were up-regulated by 93.8-fold, 33.8-fold and 2.1-fold, respectively (Fig. 2G-I). We also assessed neuroinflammation. The gene expression levels of IL-1β, IL-6 and TNF-α in the brain tissue were also elevated by 11.9-fold, 1.2-fold and 9.5-fold, respectively, after LPS injection compared with controls. In addition, combined with AHH exposure, significant increases in the gene expression levels of IL-1β, IL-6 and TNF-α by 14.3-fold, 1.4-fold and 21.7-fold, respectively, were observed in the brain tissue of LPS-injected mice compared with controls (Fig. 2J-L). These data show that LPS-induced systemic inflammation rapidly aggravates the development of brain edema in mice after AHH exposure.

3.3 Enhancement of LPS-induced microglial activation and AQP-4 accumulation by AHH exposure

To quantify the severity of central nerve system (CNS) inflammation accompanying the peripheral inflammation, we measured microglial activation at 6 h after AHH exposure using Iba-1 staining as a measurement of microglial density. The total numbers of microglia in the hippocampal CA1 region and dentate gyrus (DG) were not changed in the mice exposed to AHH alone compared with the controls.

There was a significantly greater proportion of activated microglia in the CA1 and DG in the groups treated with LPS independent of whether they were exposed to AHH (Fig. 3A-C). The activation of astrocytes was evaluated by immunostaining for the astrocyte marker glial fibrillary acidic protein (GFAP). We did not observe any overall changes in GFAP immunostaining or GFAP protein levels in the brain after exposure to AHH with or without LPS treatment (Fig. 3B-D, Suppl. Fig. 1A-B). However, the expression of AQP-4, a glial membrane water channel in the brain, was markedly increased by nearly 2-fold in the brain in the group treated with LPS and AHH exposure compared with the three other groups (Fig. 3E-G). HIF signaling plays key roles in cells subjected to decreased oxygen content. Although HIF-1α is widely expressed, HIF-2α functions in endothelial cells. We found that both HIF-1α and HIF-2α were significantly up-regulated in the group treated with LPS injection and AHH exposure (Suppl. Fig. 2). At the same time, VEGF, a key molecule regulating capillary leakage that is itself regulated by HIF signaling, was up-regulated by 2-fold in the group treated with LPS injection and AHH exposure. However, LPS injection had no impact on VEGF, and the group treated with AHH exhibited a 1.3-fold up-regulation of VEGF (Fig. 3E-F). These data indicate that the combination of LPS injection and AHH exposure enhanced the glial inflammatory response and that the accumulation of AQP-4 increased water permeability; both may play an important role in the augmentation of brain edema under hypoxia.

3.4 The LPS-induced inflammatory response rapidly accelerated the disruption of the BBB under AHH exposure

Cerebral edema is a consequence of structural and functional disruption of the BBB that is an early and prominent feature of CNS inflammation. To further investigate the potential mechanism of inflammation in the development of hypoxic brain injury, we assessed whether LPS-induced systemic inflammation accelerated the disruption of the BBB under hypoxia. We first quantified BBB permeability using Evans blue dye. There was a marked increase in the concentration of Evans blue in the brain extracts of mice in the group treated with LPS injection and AHH exposure (Fig. 4A-B). The function of the BBB is maintained by tight junctions, and we observed the structure of tight junctions using transmission electron microscopy. High-density shadows between endothelial cells revealed intact tight junctions in the control group. LPS injection and AHH exposure did not impact the integrity of tight junctions. Mild swelling of the mitochondria was visualized in the group exposed to AHH.

When LPS injection and AHH were combined, BBB disruption was observed; the basal lamina exhibited lower electron density, and dilated extracellular spaces surrounding the capillaries indicated perivascular edema. In addition to these changes, the opening of tight junctions between the endothelial cells was significantly increased (Fig. 4C). We further evaluated the molecular changes in tight junction proteins and adherens junctions. Although ZO-1 and claudin-5 did not exhibit marked changes, occludin and VE-cadherin were down-regulated by 70% and 50%, respectively, in mice that received LPS injection combined with AHH exposure (Fig. 4D-H). These results suggest that LPS-induced inflammation accelerated hypoxic brain injury by increasing BBB permeability and disrupting the tight junctions in mice.

3.5 AHH exposure combined with LPS injection significantly induced neuronal injury

The BBB separates the brain parenchyma from the circulatory and immune system, which shields the brain from blood-borne toxins and is essential for the stability of a homeostatic environment. Different staining methods and transgenic mice were used to evaluate brain injury. HE staining revealed no significant morphological changes in the group treated with LPS compared with the control group. The group treated with AHH exposure showed a widened blood vessel diameter. The group treated with LPS injection and AHH exposure showed some darkly stained pyknotic nuclei and lightly stained cytoplasm, which indicates cell death and swelling (Fig. 5A). Nissl staining showed that the group treated with LPS injection and AHH exposure exhibited the least staining of the groups, which indicates neuronal injury (Fig. 5B). Thy1-YFP transgenic mice were then used to evaluate morphological changes in projection neurons. As shown in Fig. 5C, LPS injection did not influence projection neurons, whereas AHH exposure induced the loss of YFP-positive neurons in the hippocampus. When mice were treated with LPS injection and exposed to AHH, the number of YFP-positive projection neurons significantly decreased. These data indicate that the combination of LPS injection and AHH exposure significantly induced neurological injury.

3.6 LPS-induced inflammation induced cognitive dysfunction and dyskinesia under AHH exposure

High altitude cerebral edema is characterized by ataxia and decreased consciousness. Thus, we evaluated the cognitive and motor abilities of mice subjected to LPS injection, AHH exposure or both using the Morris water maze and Rota-rod tests. After five days of training, the mice were subjected to

different treatments on the 6th day. Each mouse was placed in a pool and tracked for 60 s to measure spatial learning and memory. The mice in the group treated with LPS injection and AHH exposure took much longer than the controls to find the hidden platform. The number of platform crossings, path lengths and the time in the target quadrant also decreased significantly. The mice treated with LPS injection or AHH exposure alone showed no changes in these indexes (Fig. 6B-E). The mice treated with LPS injection swam much more slowly than the mice in the other two groups, regardless of whether they were treated with AHH exposure (Fig. 6F). The Rota-rod test was employed to evaluate the motor abilities of the mice. Although the mice in the group treated with LPS injection and exposed to AHH fell off the rod much earlier and at a slower rotational speed than the control mice, the mice in the group treated with LPS injection or AHH exposure alone showed no change compared with the control group (Fig. 6G-H). These data suggest that LPS-induce inflammation induced cognitive dysfunction and dyskinesia in the mice exposed to AHH.

4. Discussion

In this study, we found that hypoxia augments LPS-induced inflammation and triggers HACE, and we illuminated the potential mechanisms by which AHH exposure induces cerebral edema in mice (Fig. 7). We demonstrated that the inflammatory response accelerates the occurrence and development of brain edema under AHH exposure, which is associated with increased BBB permeability, microglial activation, and the enhanced expression of the water channel AQP-4, ultimately leading to impaired cognitive and motor function in mice. These findings prove that the inflammatory response is a key determinant in the occurrence, progression, and acute outcomes of HACE and suggest a potential therapeutic target for the treatment of various pathological states that are involved in hypoxic brain injury.

Inflammation plays a role in the generation and development of many diseases. As the main reservoir of bacteria and endotoxins, intestinal tract dysfunction also exerts vital effects in many diseases (Luo et al., 2012). However, the incidence of digestive system disease has been reported to be high in those living at high altitude (Recavarren et al., 2005). In a recently published study, scientists found that bifidobacteria and species belonging to the Atopobium, Coriobacterium and *Eggerthella lenta* groups decreased, whereas potential pathogenic bacteria of the gamma subdivision of Proteobacteria and specific Enterobacteriaceae such as *Escherichia coli* increased after high altitude

exposure above 5,000 m (Kleessen et al., 2005). An investigation conducted by Murdoch also showed that those with respiratory or gastrointestinal infections during ascent to high altitude have a higher incidence of AMS. The author also found that the frequency of infectious symptoms was positively related to Lake Louise scores (Murdoch, 1995). A growing body of evidence shows that infection and inflammation play pivotal roles in altitude-related illnesses (Bailey et al., 2004).

Rodent species are particularly insensitive to hypoxia exposure. AHH exposure does not induce pro-inflammatory cytokine release in the short-term. As hypobaric hypoxia exposure is prolonged, pro-inflammatory cytokines in the plasma and brain are up-regulated. LPS is a strong inducer of pro-inflammatory cytokines. When animals receive low-dose LPS injections, AHH exposure rapidly augments the expression and release of pro-inflammatory cytokines. In a study by Jian et al., cytokine expression induced by LPS was amplified by 1% O_2 exposure in periodontal ligament cells (Jian et al., 2014). When neuroinflammation is induced, pro-inflammatory cytokines are the major factors that cause BBB disruption. It is well known that TNF-α, IFN-γ, IL-1β, and IL-6 exposure induce the down-regulation of tight junctions (Varatharaj and Galea., 2016; Erickson et al., 2012). This phenomenon is induced by the over-production of reactive oxygen species (ROS), COX-2 and PG and the inhibition of SHH (Almutairi et al., 2016). Additionally, pro-inflammatory cytokines can up-regulate the expression of VEGF, a key regulator of BBB permeability (Ahmed-Jushuf et al., 2016), which was also observed in our experiment. In addition, AQP-4 was up-regulated, further indicating the onset of cerebral edema.

The BBB separates the CNS and the peripheral circulatory system, thus maintaining stability of the homeostatic environment, which is the basis of the normal function of neurons (Abbott, 2013). The BBB is maintained by tight junctions between adjacent endothelial cells. Tight junctions include members of the claudin family, occludin and junctional adhesive molecules (Stamatovic et al., 2016), of which claudin-5 and occludin are the most important and widely researched. These molecules are linked to the cytoskeleton by ZO. Adherens junctions also constitute junctional complexes and play important roles in BBB stability (Chow and Gu. 2015). In our experiment, the opening of tight junctions was prominent in the group treated with LPS injection and exposed to AHH. The tight junction protein occludin and the adherens junction protein VE-cadherin were also significantly down-regulated only in the group treated with LPS injection and exposed to AHH. In the study by Kangwantas et al., the authors found that both oxygen glucose deprivation (OGD) and IL-1β treatment

induced the translocation of tight junction proteins from the cytomembrane, but the transepithelial electric resistance (TEER) was not changed. When OGD and IL-1β exposure were combined, the translocation of tight junctions was much more significant, and TEER also decreased significantly, which reflected the disruption of the BBB (Kangwantas et al., 2016). Luo also reported that rats exposed to hypoxia and LPS injection exhibit significant bacterial translocation in the intestinal tract and sub-epithelial tight junction opening (Luo et al., 2012). These experiments all show that inflammation is amplified by hypoxia in conjunction with tight junction opening in both cells and animals.

LPS injection is widely used to model systemic inflammation. Bacterial endotoxins exert strong effects on the immune neuroendocrine network and induce profound physiological and behavioral alterations that include fever, anorexia, anhedonia, lethargy, ptosis, and depression of both exploration and social behavior, among others (Gasparotto et al., 2007). A medium-dose LPS injection (5 mg/kg) reversibly impaired spatial learning and memory. However, the impairments induced by high-dose injections (10 mg/kg) of LPS were irreversible (Bian et al.,2013). Physiological parameters such as body weight, blood pressure and heart rate were not influenced in rats that received low-dose LPS injections (Krizak et al., 2016). Furthermore, motor abilities were not affected by low-dose LPS injections (0.5 mg/kg) in mice (Couch et al., 2016). In our experiments, we found that LPS injection reduced swimming speed but did not impair spatial memory. The combination of LPS injection and AHH exposure prolonged the latency to find the hidden platform, reduced the number of times the platform area was crossed, and reduced the time and path length in the target quadrant. The Rota-rod test showed that reduced motor ability appeared only in the group treated with LPS injection and exposed to AHH. These findings resembled those reported by Gasparotto et al. in which low dose LPS injections exacerbated stress-induced depressive-like behaviors (Gasparotto et al., 2007).

In this study, our results indicated that the systemic inflammatory status is a key determinant of acute outcomes and the long-term progress of brain edema in high altitude hypoxia. Thus, we propose herein a mechanistic explanation for the relationship between inflammation and brain edema under hypoxia and provide a novel potential therapeutic target for the treatment of HACE. The effects of anti-inflammation in high altitude-induced brain injury need to be addressed in future studies.

Abbreviations

ADC: apparent diffusion coefficient; AMS: acute mountain sickness; AQP-4: aquaporin-4; BBB: blood brain barrier; BWC: brain water content; GFAP: astrocyte marker glial fibrillary acidic protein; HACE: high altitude cerebral edema; LPS: lipopolysaccharide; OGD: oxygen glucose deprivation; TEER: trans epithelial electric resistance; TJ: tight junction;ZO: Zonula Occludens.

Declarations

Ethics approval and consent to participate:

All study procedures involving animals were performed in accordance with the ethical standards of the Institutional Research Committee. Mice were maintained at the animal facility with free access to water and food in accordance with institutional guidelines. The Institutional Animal Care and Use Committee (IACUC) of the Academy of Beijing Medical Sciences approved all the experiments involving mice.

Consent for publication

Not applicable.

Availability of data and materials

The reproducible materials described in this manuscript, including any new software, databases and all relevant raw data, are freely available to any scientist wishing to use them, without breaching participant confidentiality.

Competing interests

The authors declare that they have no conflicts of interest.

Funding

This work was supported by grants from the Natural Science Foundation of China (Nos. 81430044 and 31370022), the Beijing Natural Science Foundation (No. 5132025), and the National Basic Research Program of China (Nos. 2011CB910800 and 2012CB518200).

Authors' contributions

Yan Zhao Zhou: performed the research, analyzed the data; Xin Huang: designed the research, performed the research, analyzed the data, wrote the paper; Tong Zhao: contributed new reagents or analytic tools; Meng Qiao: contributed new reagents or analytic tools; Xingnan Zhao: analyzed the data; Ming Zhao: analyzed the data, contributed new reagents or analytic tools; Lun Xu: contributed new reagents or analytic tools; Yongqi Zhao: analyzed the data; Liying Wu: contributed new reagents or analytic tools; Kuiwu Wu: contributed new reagents or analytic tools; Ruoli Chen: provided reagents; Ming Fan: designed the research, analyzed the data, wrote the paper; and Lingling Zhu: designed the

research, contributed new reagents or analytic tools, analyzed the data, wrote the paper.

Acknowledgements

This work was supported by grants from the Natural Science Foundation of China (Nos. 81430044 and 31370022), the Beijing Natural Science Foundation (No. 5132025), and the National Basic Research Program of China (Nos. 2011CB910800 and 2012CB518200).

References

Ahmed-Jushuf F, Jiwa NS, Arwani AS, Foot P, Bridges LR, Kalaria RN, Esiri MM, Hainsworth AH., 2016. Age-dependent expression of VEGFR2 in deep brain arteries in small vessel disease, CADASIL, and healthy brains. Neurobiol Aging. 42:110-5.

Almutairi MM, Gong C, Xu YG, Chang Y, Shi H., 2016. Factors controlling permeability of the blood-brain barrier. Cell Mol Life Sci. 73(1):57-77.

Bailey DM, Kleger GR, Holzgraefe M, Ballmer PE, Bärtsch P., 2004. Pathophysiological significance of peroxidative stress, neuronal damage, and membrane permeability in acute mountain sickness. 96(4):1459-63.

Bailey DM, Bärtsch P, Knauth M, Baumgartner RW., 2009.Emerging concepts in acute mountain sickness and high-altitude cerebral edema: from the molecular to themorphological. Cell Mol Life Sci. 66(22):3583-94.

Bärtsch P, Swenson ER.,2013 Acute high-altitude illnesses. N Engl J Med. 24;369(17):1666-7.

Bian Y, Zhao X, Li M, Zeng S, Zhao B., 2013. Various roles of astrocytes during recovery from repeated exposure to different doses of lipopolysaccharide. Behav Brain Res. 253:253-61.

Carpenter TC, Reeves JT, Durmowicz AG., 1998. Viral respiratory infection increases susceptibility of young rats to hypoxia-induced pulmonary edema. J Appl Physiol. 84(3):1048-54.

Chow BW, Gu C., 2015. The molecular constituents of the blood-brain barrier. Trends Neurosci. 38(10):598-608.

Couch Y, Trofimov A, Markova N, Nikolenko V, Steinbusch HW, Chekhonin V, Schroeter C, Lesch KP, Anthony DC, Strekalova T., 2016.

Low-dose lipopolysaccharide (LPS) inhibits aggressive and augments depressive behaviours in a chronicmild stress model in mice. J Neuroinflammation. 13(1):108. doi: 10.1186/s12974-016-0572-0.

Dickinson JG, 1979. Sever acute mountain sickness. Postgrad Medd J. 55(645):454-60

Eide RP 3rd, Asplund CA. 2012. Altitude illness: update on prevention and treatment. Curr Sports Med Rep. 11(3):124-30.

Durmowicz AG, Noordeweir E, Nicholas R, Reeves JT., 1997. Inflammatory processes may predispose children to high-altitude pulmonary edema. J Pediatr. 130(5):838-40.

Erickson MA, Dohi K, Banks WA., 2012. Neuroinflammation: a common pathway in CNS diseases as mediated at the blood-brain barrier. Neuroimmunomodulation. 19(2):121-30.

Gallagher SA, Hackett PH.，2004. High-altitude illness.Emerg Med Clin North Am. 22(2):329-55, viii.

Gasparotto OC, Carobrez SG, Bohus BG., 2007. Effects of LPS on the behavioural stress response of genetically selected aggressive and nonaggressive wild house mice. Behav Brain Res. 183(1):52-9.

Guo G, Zhu G, Sun W, Yin C, Ren X, Wang T, Liu M., 2014. Association of arterial oxygen saturation and acute mountain sickness susceptibility: a meta-analysis. Cell Biochem Biophys. 70(2):1427-32.

Hackett PH, Roach RC.,2001. High-altitude illness. N Engl J Med. 345(2):107-14.

Huang X, Zhou Y, Zhao T, Han X, Qiao M, Ding X, Li D, Wu L, Wu K, Zhu LL, Fan M., 2015. A method for establishing the high-altitude cerebral edema (HACE) model by acute hypobaric hypoxia in adult mice. J Neurosci Methods. 245:178-81.

Jian C, Li C, Ren Y, He Y, Li Y, Feng X, Zhang G, Tan Y., 2014. Hypoxia augments lipopolysaccharide-induced cytokine expression in periodontal ligament cells. Inflammation. 37(5):1413-23.

Kangwantas K, Pinteaux E, Penny J., 2016. The extracellular matrix protein laminin-10 promotes blood-brain barrier repair after hypoxia andinfla mmation in vitro. J Neuroinflammation. 13:25. doi: 10.1186/s12974-016-0495-9.

Krizak J, Frimmel K, Bernatova I, Navarova J, Sotnikova R, Okruhlicova L., 2016. The effect of omega- 3 polyunsaturated fatty acids on endothelial tight junction occludin expression in rataorta during lipopolysaccharide-induced inflammation. Iran J Basic Med Sci. 19(3):290-9.

Kleessen B, Schroedl W, Stueck M, Richter A, Rieck O, Krueger M., 2005. Microbial and immunological responses relative to high-altitude exposure in mountaineers. Med Sci Sports Exerc. 37(8):1313-8.

Luo H, Guo P, Zhou Q., 2012. Role of TLR4/NF-κB in damage to intestinal mucosa barrier function and bacterial translocation in rats exposed to hypoxia. PLoS One. 7(10):e46291. doi: 10.1371/journal.pone.0046291.

MacInnis MJ, Koehle MS, Rupert JL.,2010. Evidence for a genetic basis for altitude illness: 2010 update. High Alt Med Biol. 11(4):349-68.

Morris M, Hamto P, Adame A, Devidze N, Masliah E, Mucke L., 2013. Age-appropriate cognition and subtle dopamine-independent motor deficits in aged tau knockout mice. Neurobiol Aging. 34(6):1523-9.

Murdoch DR., 1995. Symptoms of infection and altitude illness among hikers in the Mount Everest region of Nepal. Aviat Space Environ Med. 66(2):148-51.

Netzer N, Strohl K, Faulhaber M, Gatterer H, Burtscher M., 2013. Hypoxia-related altitude illnesses. J Travel Med. 20(4):247-55.

Recavarren-Arce S, Ramirez-Ramos A, Gilman RH, Chinga-Alayo E, Watanabe-Yamamoto J, Rodriguez-Ulloa C, Miyagui J, Passaro DJ, Eza D., 2005. Severe gastritis in the Peruvian Andes. Histopathology.46(4):374-9.

Rietschel ET, Kirikae T, Schade FU, Mamat U, Schmidt G, Loppnow H, Ulmer AJ, Zähringer U, Seydel U, Di Padova F,, 1994. Bacterial endotoxin: molecular relationships of structure to activity and function. FASEB J. 8(2):217-25.

Rodway GW, Hoffman LA, Sanders MH.,2003. High-altitude-related disorders--Part I: Pathophysiology, differential diagnosis, and treatment. Heart Lung. 32(6):353-9.

Song TT, Bi YH, Gao YQ, Huang R, Hao K, Xu G, Tang JW, Ma ZQ, Kong FP, Coote JH, Chen XQ, Du JZ., 2016.

Systemic pro-inflammatory response facilitates the development of cerebral edema during short hypoxi a. J Neuroinflammation. 11;13(1):63. doi: 10.1186/s12974-016-0528-4.

Stamatovic SM, Johnson AM, Keep RF, Andjelkovic AV., 2016. Junctional proteins of the blood-brain barrier: New insights into function and dysfunction. Tissue Barriers. 26;4(1):e1154641. doi: 10.1080/21688370.2016.1154641.

Varatharaj A, Galea I., 2016. The blood-brain barrier in systemic inflammation. Brain Behav Immun. doi: 10.1016/j.bbi.2016.03.010.

Zuo S, Ge H, Li Q, Zhang X, Hu R, Hu S, Liu X, Zhang JH, Chen Y, Feng H., 2016. Artesunate Protected Blood-Brain Barrier via Sphingosine 1 Phosphate Receptor 1/Phosphatidylinosito l 3 KinasePathway After Subarachnoid Hemorrhage in Rats. Mol Neurobiol. doi:10.1007/s12035-016-9732-6

Figure legends

Fig. 1 AHH slightly increased the levels of TNF-α, IL-1β, and IL-6 in mice within 24 h.

(A-C) The levels of TNF-α, IL-1β, and IL-6 in the serum of mice after exposure to AHH at different time points were determined by ELISA. (D-F) The mRNA expression levels of TNF-α, IL-1β, and IL-6 in the hippocampus of mice after exposure to AHH at different time points were determined by qPCR. G. Changes in BWC in mice after AHH exposure at different time points within 24 h. (The data are presented as the mean ± SEM. *: $p < 0.05$ compared with the control group, **: $p < 0.01$ compared with the control group. n = 5 in each group.)

Fig. 2 LPS-induced systemic inflammatory response rapidly aggravated the development of brain edema after exposure to AHH in mice.

(A) BWC was determined using the wet/dry weight ratio in mice treated with different dosages of LPS with or without AHH exposure. (B) Representative image of a mouse brain that underwent a combination of AHH exposure and LPS treatment. (C) The ADC values determined by MRI after a combination of AHH exposure and LPS treatment were significantly increased compared with the control group. (D-F) TNF-α, IL-1β, and IL-6 levels in the serum of mice were measured by ELISA

following LPS injection, AHH exposure or a combination of both treatments. (G-I) The mRNA expression levels of MCP-1, ICAM, and VCAM in the hippocampus of mice were determined by qPCR following LPS injection, AHH exposure or a combination of both treatments. (J-L) The mRNA expression levels of TNF-α, IL-1β, and IL-6 in the hippocampus of mice were determined by qPCR following LPS injection, AHH exposure or a combination of both treatments. (The data are presented as the mean ± SEM. *: $p < 0.05$ compared with the control group, **: $p < 0.01$ compared with the control group. n = 5 in each group.)

Fig. 3 Enhancement of LPS-induced microglia activation and AQP-4 expression by AHH exposure

(A) Representative image of microglia activation in the brains after the different treatments. (B) Representative image of astrocyte activation in the brain after the different treatments. (C) Microglia were activated in the group treated with LPS injection and in the group treated with the combination of LPS injection and AHH exposure. (D) GFAP expression was not influenced by the different treatments. (E-G) The expression levels of VEGF and AQP-4 were significantly up-regulated in the group treated with the combination of LPS injection and AHH exposure. (The data are presented as the mean ± SEM. *: $p < 0.05$ compared with the control group, **: $p < 0.01$ compared with the control group. n = 3 in each group.)

Fig. 4 Increased permeability of the BBB after AHH exposure combined with LPS treatment

(A) Representative image of the extraction of Evan's blue in the brain after LPS injection, AHH exposure or a combination of both treatments. (B) Quantitative analysis of BBB permeability based on Evans blue dye after the different treatments. There was a marked increase in the concentration of Evans blue in the brain extracts after exposure to AHH for 6 h with LPS injection. (C) Transmission electron microscopy was utilized to detect the morphology of the tight junctions in the brain after the different treatments. (D-H) Western blot analysis showed the down-regulation of the tight junction protein Occludin and the adherens junction protein VE-Cadherin in the group treated with both LPS injection and AHH exposure. (The data are presented as the mean ± SEM. *: $p < 0.05$ compared with the control group, **: $p < 0.01$ compared with the control group. n = 3 or 5 in each group.)

Fig. 5 Neuronal injury was induced by the combination of LPS injection and AHH exposure

(A) Darkly stained pyknotic nuclei and lightly stained cytoplasm by HE staining indicate cell injury in the groups treated with the combination of LPS injection and AHH exposure. (B) Lightly stained Nissl bodies by Nissl staining indicate neuronal injury in the groups treated with the combination of LPS injection and AHH exposure. (C) Neuron and axon loss were apparent in the group treated with the combination of LPS injection and AHH exposure as observed in Thy1-YFP transgenic mice.

Fig. 6 Cognitive and motor dysfunction were induced by the combination of LPS injection and AHH exposure

(A) Mice were trained to find the hidden platform under the water. (B) The time to find the hidden platform under the water was longer in the group of mice treated with the combination of LPS injection and AHH exposure. (C) The number of platform entries was significantly decreased in the group treated with the combination of LPS injection and AHH exposure. (D) Path length in the target quadrant was significantly decreased in the group treated with the combination of LPS injection and AHH exposure. (E) The time spent in the target quadrant was significantly decreased in the group treated with the combination of LPS injection and AHH exposure. (F) Swimming speed was decreased in the groups treated with LPS injection with or without AHH exposure. (G) The time at which the mice fell off the rolling rod was significantly decreased in the group treated with the combination of LPS injection and AHH exposure. (H) The speed of the rotating rod when the mice fell off was significantly decreased in the group treated with the combination of LPS injection and AHH exposure. (The data are presented as the mean ± SEM. *: $p < 0.05$ compared with the control group, **: $p < 0.01$ compared with the control group. n = 8 or 10 in each group.)

Fig. 7 Model of how hypoxia augments LPS-induced inflammation and triggers high altitude cerebral edema.

We demonstrated that the inflammatory response accelerates the occurrence and development of brain edema under AHH exposure, which is associated with increased BBB permeability, microglial activation, and the enhanced expression of the water channel AQP-4, ultimately leading to impaired cognitive and motor function in mice.

Suppl. Fig. 1: expression of GFAP was not affected upon either treatment. A-B: content of GFAP in each group didn't get changed. (The data are presented as the mean ± SEM. n=3 in each group)

Suppl. Fig. 2: HIF signaling was activated significantly in group treated by LPS-injection and hypobaric hypoxia exposure A-C: HIF-1α and HIF-2α were up regulated in group treated by LPS-injection and hypobaric hypoxia exposure D-F. ET-1, HO-1, EPO, VEGF were up-regulated in group treated by LPS-injection and hypobaric hypoxia exposure. (The data are presented as the mean ± SEM. *: $p < 0.05$ compared with the control group, **: $p < 0.01$ compared with the control group. n=3 in each group)

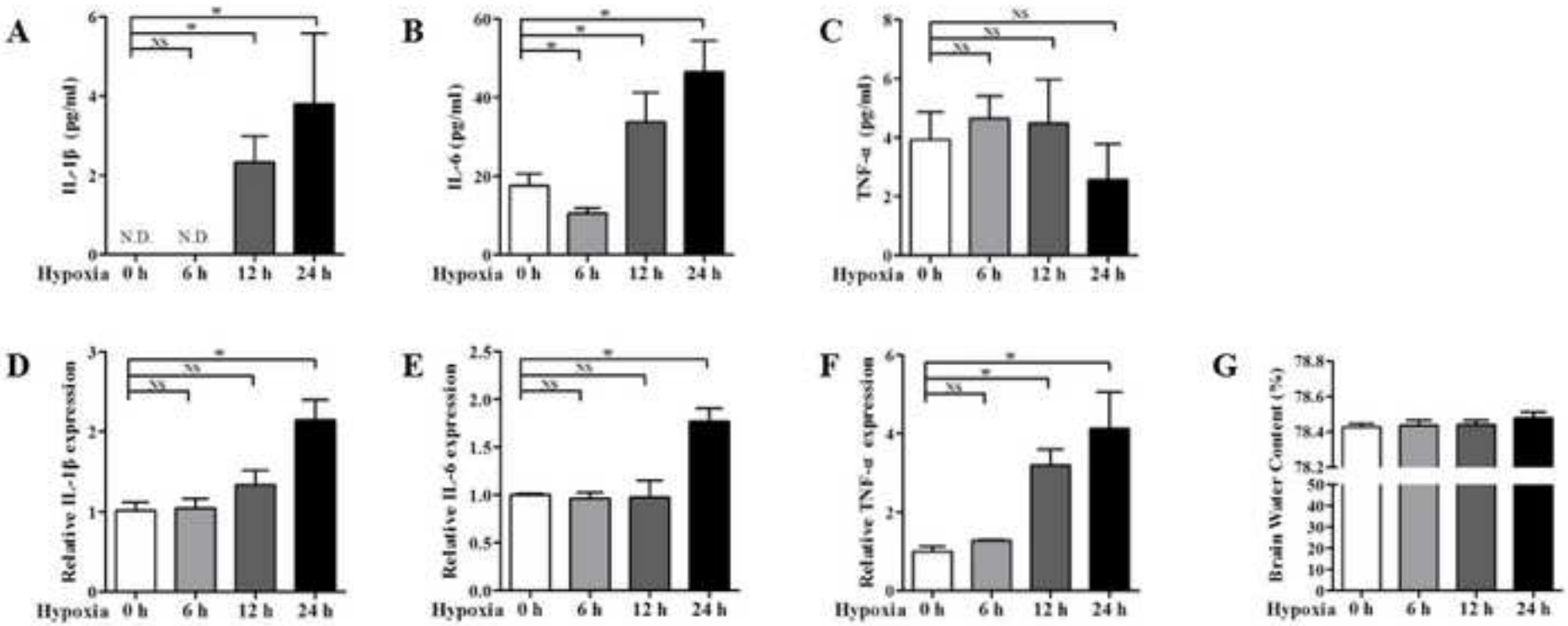

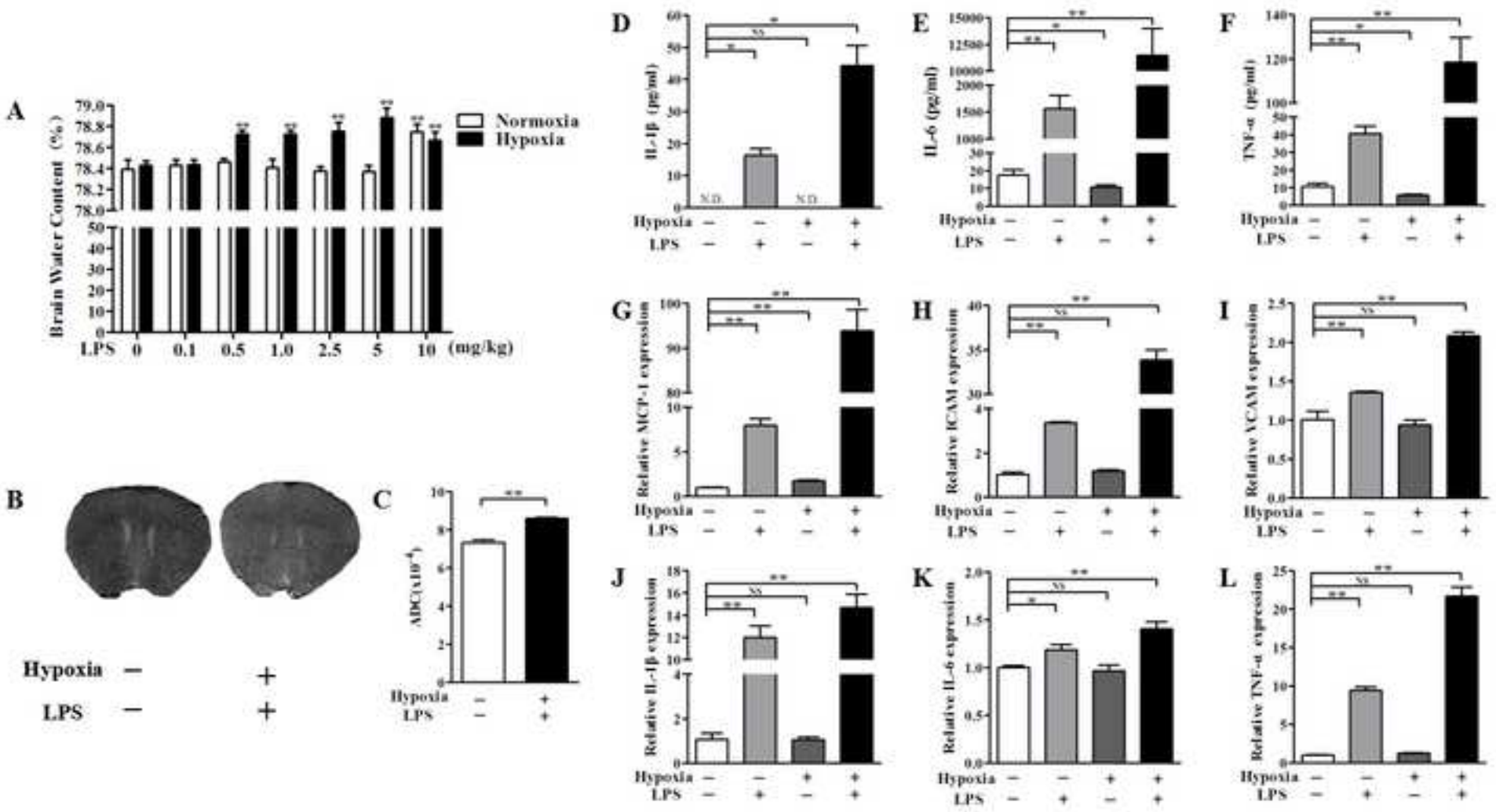

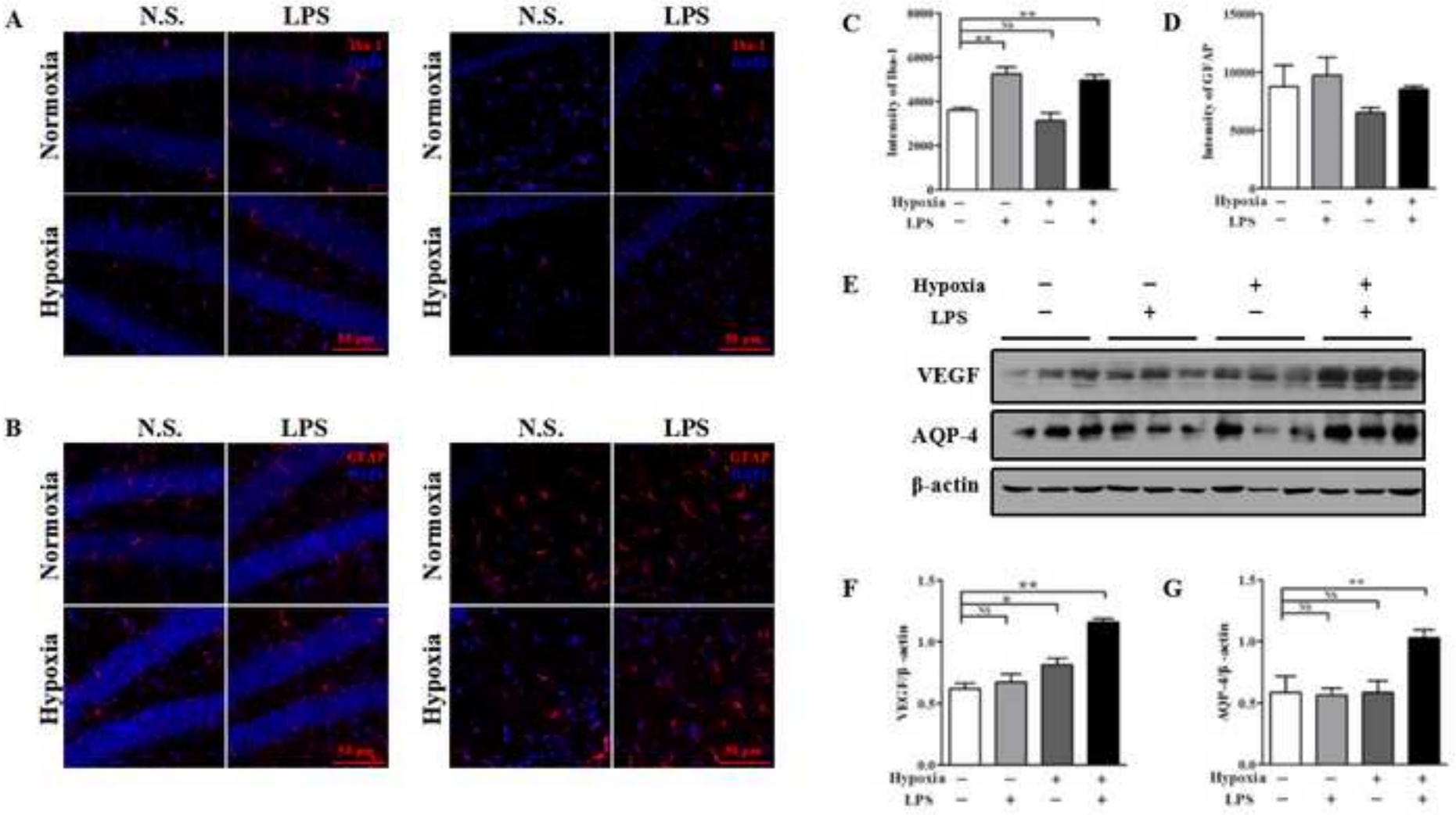

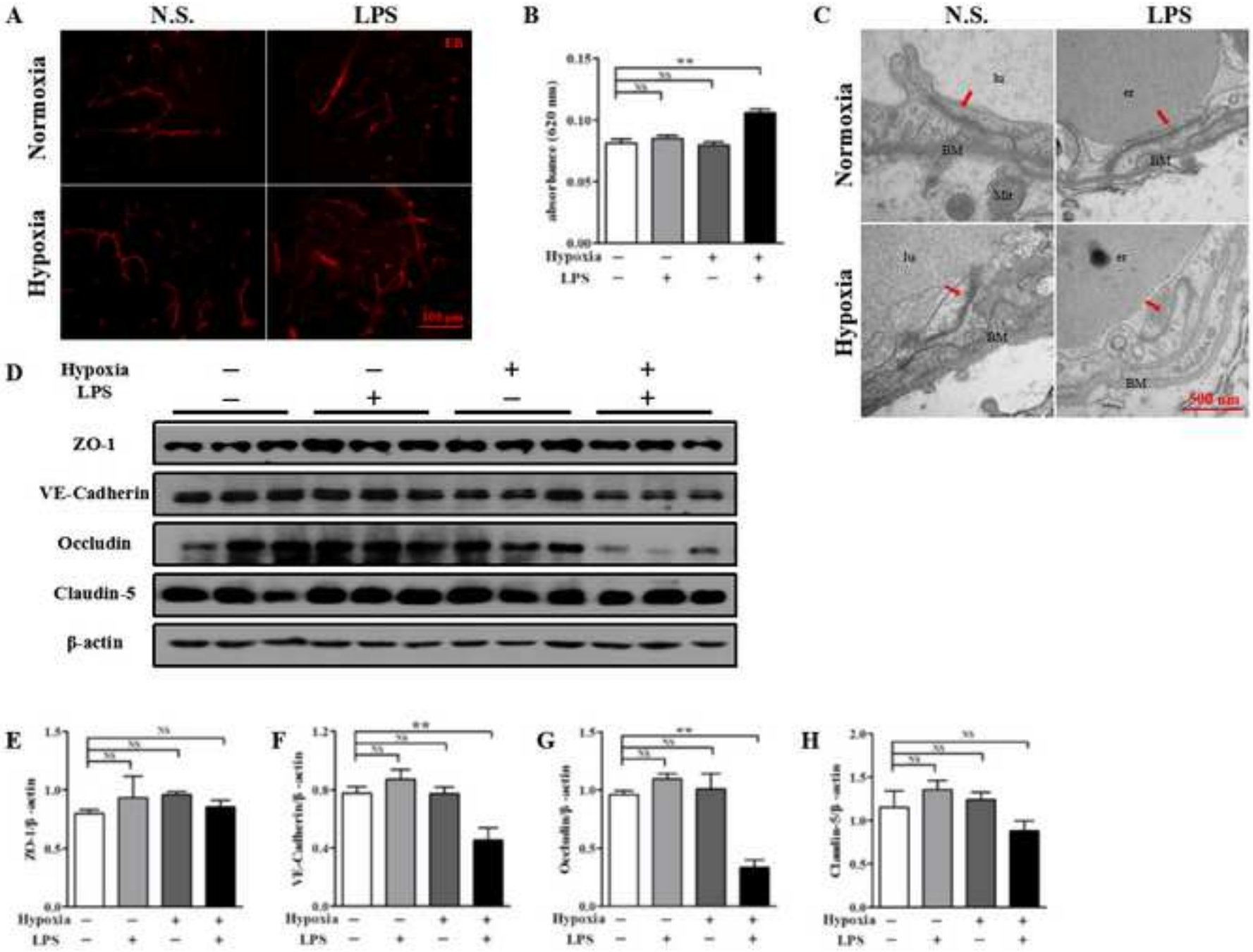

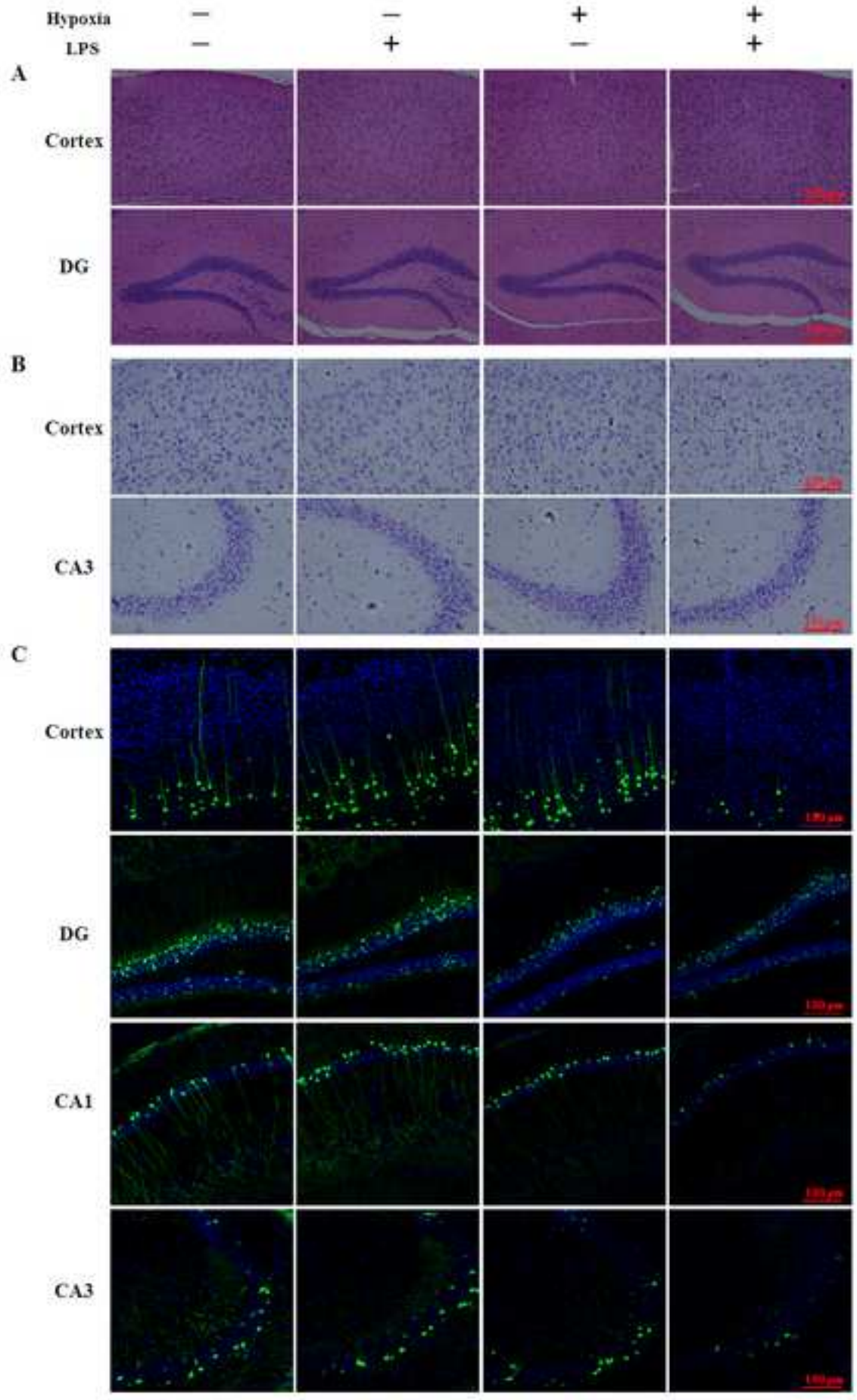

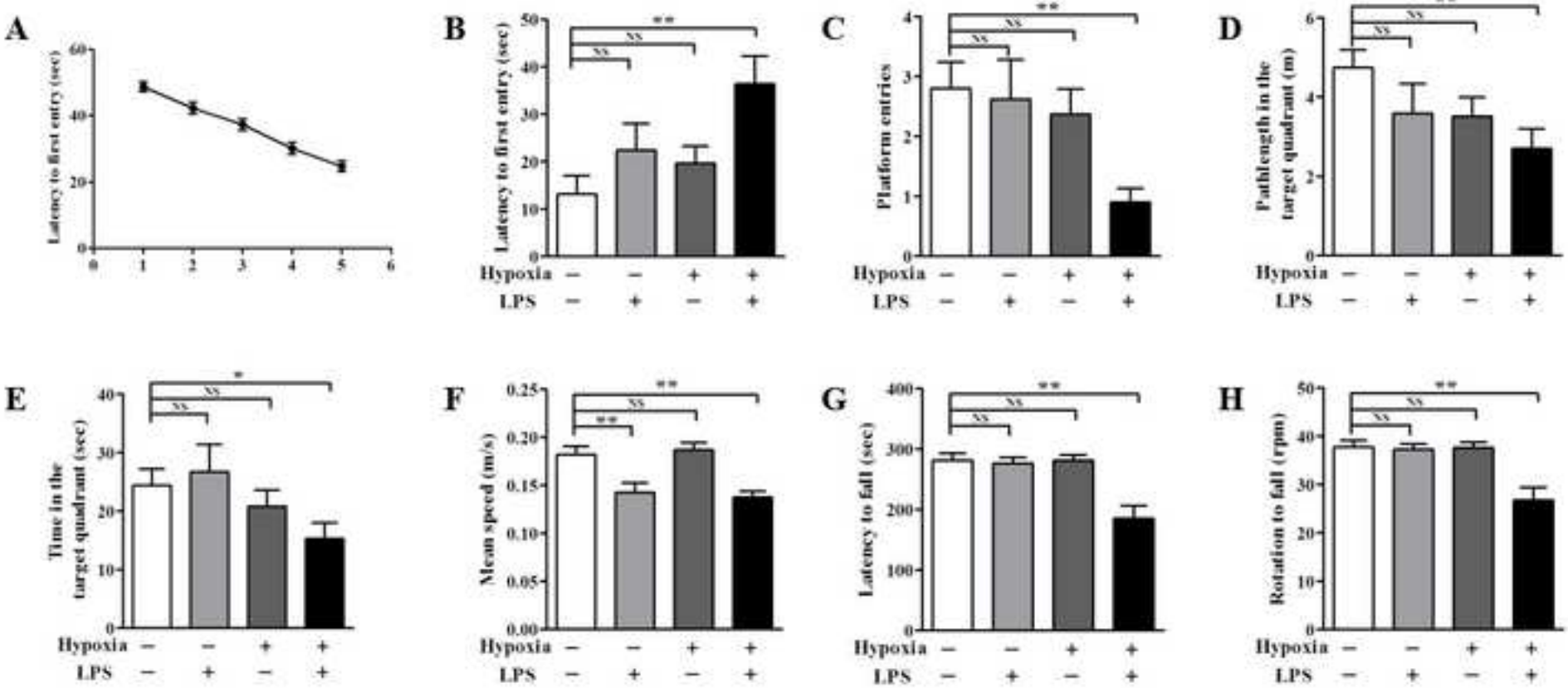

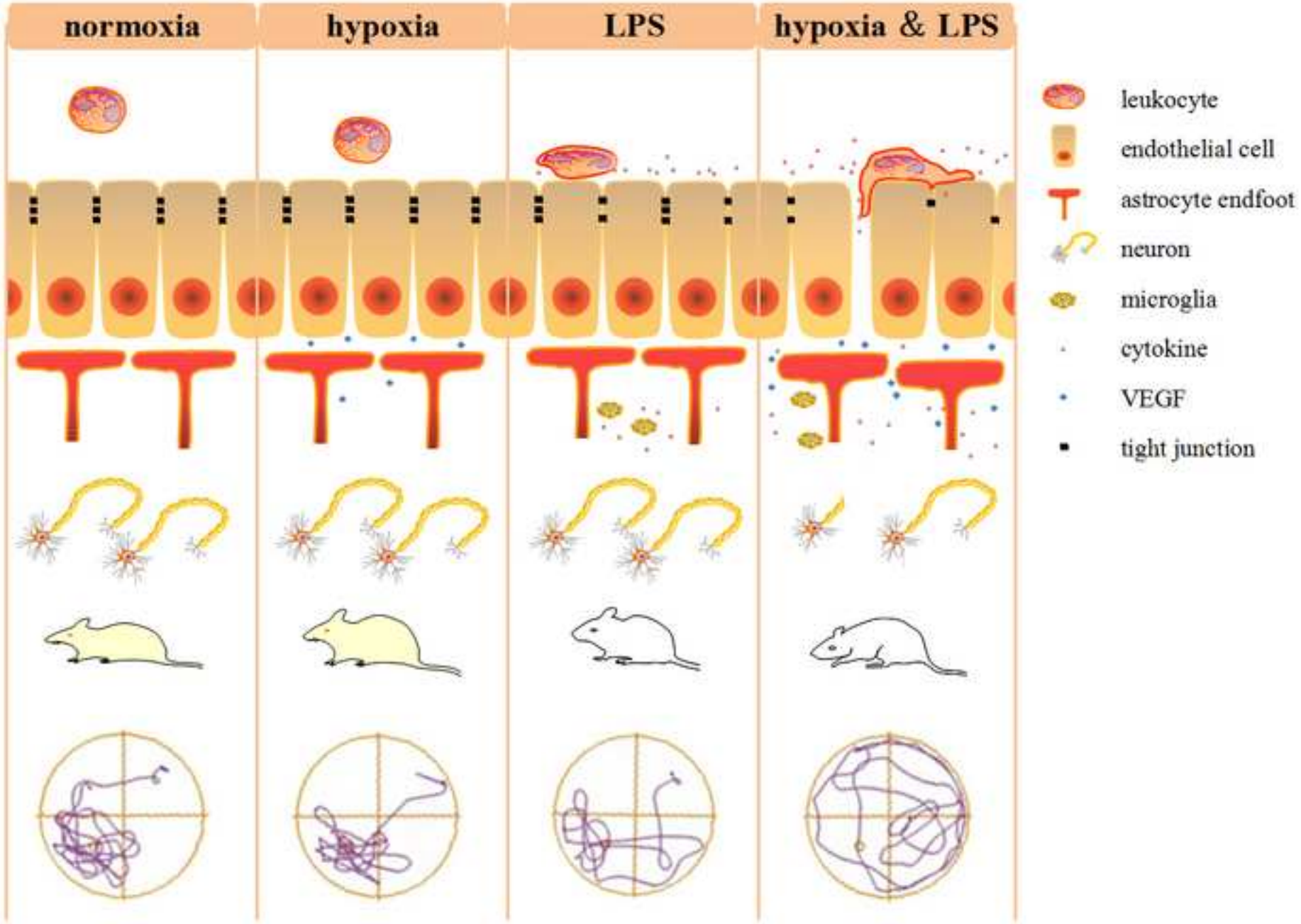

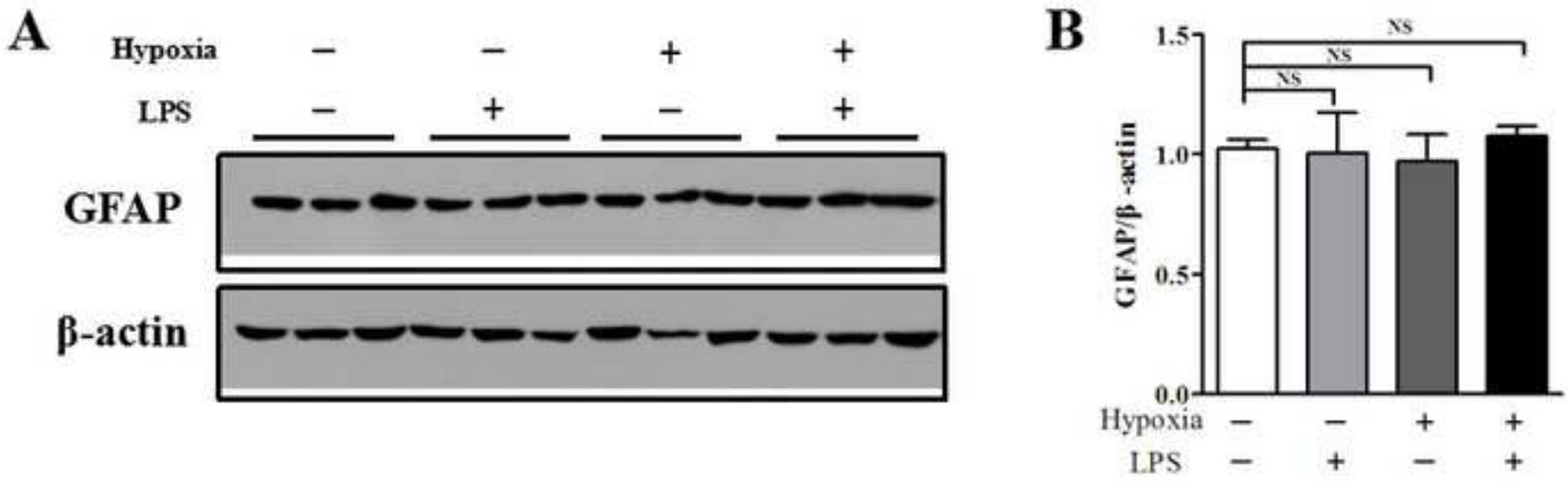

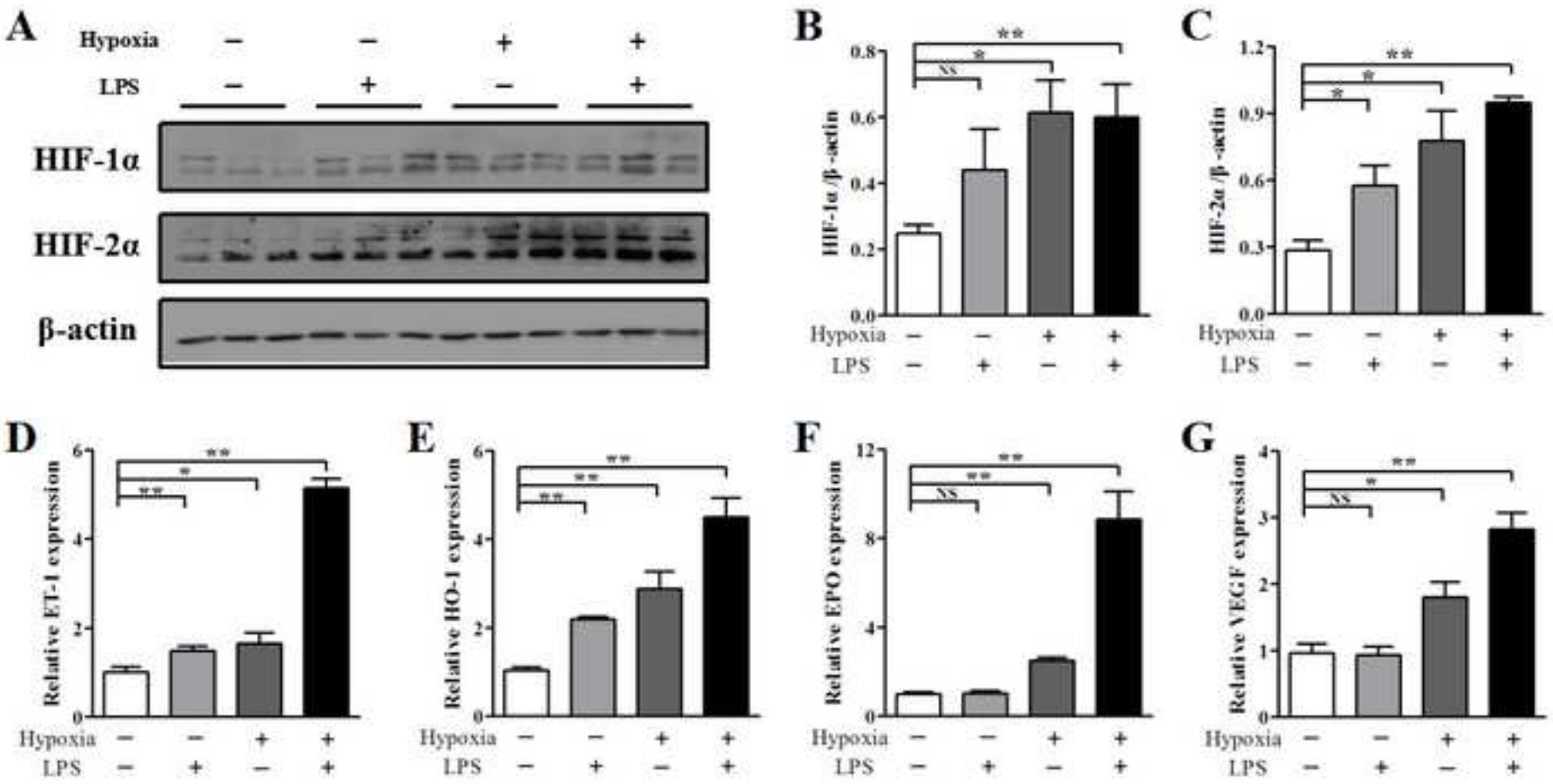

1. Inflammation may play vital roles in high altitude cerebral edema is proposed.
2.Hypoixa augments LPS-induced systemic inflammation and neuroinflammation.
3.combination of hypoxia exposure and LPS injection rapidly induces cerebral edema.
4.combination of hypoxia exposure and LPS injection induces blood-brain barrier leakage by disrupting tight junctions.
5.combination of hypoxia exposure and LPS injection induces cognitive and motor dysfunction.